Impact of Human-Centered Vestibular System Model for Motion Control in a Driving Simulator

Carolina Rengifo, Jean-Rémy Chardonnet, *Member, IEEE*, Hakim Mohellebi, and Andras Kemeny

***Abstract*—This study presents a driving simulator experiment to evaluate three different motion cueing algorithms based on model predictive control. The difference among these motion strategies lies in the type of mathematical model used. The first one contains only the dynamic model of the platform, while the others integrate additionally two different vestibular system models. We compare these three strategies to discuss the tradeoffs when including a vestibular system model in the control loop from the user's viewpoint. The study is conducted in autonomous mode and in free driving mode, as both play an important role in motion cueing validation. A total of 38 individuals participated in the experiment; 19 drove the simulator in free driving mode and the remaining using the autonomous driving mode. For both driving modes, substantial differences is observed. The analysis shows that one of the vestibular system models is suitable for driving simulators, as it thoroughly restores high-frequency accelerations and is well noted by the participants, especially those in the free driving mode. Further tests are needed to analyze the advantages of integrating the chosen vestibular system model in the control design for motion cueing algorithms. Regarding the autonomous mode, further research is needed to examine the influence of the vestibular system model on the motion performance, as the behavior of the autonomous model may implicitly interfere with subjective assessments.**

***Index Terms*—Autonomous driving (AD), driving simulators (DSs), human motion perception, model predictive control (MPC), motion cueing algorithms.**

I. Introduction

NOWADAYS most important driving simulation challenges are in autonomous vehicle research and advanced driver assistance systems validation since they require massive testing in normal, risky, and expensive situations. Also, enabling cars to generate driving behaviors while keeping the driver safe is a difficult and demanding effort task. Therefore, driving simulators (DSs) are a powerful tool for testing human behavior in safe, critical, and cost-effective scenarios. However, the validity of these technologies in simulation is heavily depending on the DS performance as the relationship between simulator fidelity and validity is not straightforward [1]. Therefore, it is necessary to select the DS's characteristics carefully.

Since motion signals cannot be sent directly from the vehicle model to the DS due to its limits, motion restitution is one of the most critical characteristics regarding driving simulation. To overcome this issue, motion cueing algorithms (MCAs) are implemented [2]. Several efforts have been made in MCA development in order to increase simulation realism and reduce the well-known simulator sickness induced by conflicting effects among subsystems. One of the approaches aiming at solving these problems has been to integrate human motion perception into the control design. Most MCAs use human perceptive system information to restore additional linear acceleration while tilting the platform cockpit [3]–[6]. This is a well-known technique named tilt coordination.

Some optimization-based techniques such as optimal [7] or model predictive control (MPC) [8] in MCA, integrate the vestibular system's mathematical model into the control design to minimize the error between the perceived vehicle and simulator motion cues. Located inside the inner ear, the vestibular system comprises the otolith organs and the semicircular canals, which act as sensors for linear and rotational accelerations, respectively. The literature provides several vestibular system models [9]. However, when designing MCAs, only two models are mostly employed in a model reference and control theory context. The first one includes both, the semicircular canals [10] and the otolith organs model [11]. This model has been used in numerous studies [8], [12]–[18]. The second model proposed by [19] also integrates both models, but is more recent and is the most used model among MCAs [20]–[25]. Although most researchers suggest that using an accurate vestibular sensor model improves motion restitution quality, its implementation without any experimental test is not obvious. In fact, some authors continue to design MCAs without considering any human vestibular sensor model [26], [27]. Furthermore, the integration of this model makes the control design more complex and increases the optimization time as the number of states in the system increases.

Manuscript received October 10, 2019; revised March 9, 2020, October 24, 2020, January 23, 2021, and April 18, 2021; accepted June 24, 2021. This work was supported in part by Renault's group and the ANRT (National Research and Technology Agency). This article was recommended by Associate Editor J. de Winter. *(Corresponding author: Carolina Rengifo.)*

Carolina Rengifo is with Renault, 78288 Guyancourt, France, and also with the LISPEN EA7515, Arts et Métiers, HESAM, Université Bourgogne Franche-Comté and Institut Image, 71100 Chalon-sur-Saône, France (e-mail: carolina.rengifo.c@gmail.com).

Jean-Rémy Chardonnet is with the LISPEN EA7515, Arts et Métiers, HESAM, Université Bourgogne Franche-Comté and Institut Image, 71100 Chalon-sur-Saône, France (e-mail: Jean-Remy.CHARDONNET@ensam.eu).

Hakim Mohellebi and Andras Kemeny are with Renault, 78288 Guyancourt, France (e-mail: hakim.mohellebi@renault.com; andras.kemeny@renault.com).

Color versions of one or more figures in this article are available at https://doi.org/10.1109/THMS.2021.3102506.

To the best of authors' knowledge, no comparison has been made between integrating a vestibular system model or just using the dynamics of the platform into the MCA for a DS. In addition, the two vestibular system models presented earlier have not been compared in experimental tests. Therefore, this article proposes to evaluate three different motion strategies that depend directly on the mathematical model used in the control design. The first configuration contains only the platform dynamic model without any vestibular system model, the second one integrates Young–Oman/Meiry's model [10], [11], while the third one uses the Telban and Cardullo's model [19]. Throughout this article, they will be called M0, M1, and M2, respectively.

In this regard, the main objective of this study is to validate the mathematical model used in MPC-based MCAs to improve driver-in-the-loop immersion and motion perception in a DS. For this purpose, we show the mathematical model impact on motion perception; we compare the M0, M1, and M2 configurations from an experimental perspective in both autonomous driving (AD) and free driving (FD) modes.

The rest of this article is organized as follows. Section II goes over modeling of the different motion strategies using an MPC technique, followed by a comparison between them in Section III. Section IV presents the experimental methodology and procedure. Section V discusses the experimental results. Finally, Section VI concludes the article.

II. Control Strategy Modeling

MPC-based MCA aims at reproducing as best as possible the vehicle signals by minimizing the error between the desired driver acceleration signals and the simulator response while respecting constraints within a prediction window. However, in the presence of sustained accelerations, the platform working space is limited and its physical limits are reached quickly. Hence, in order to improve the tracking task and maximize driver motion perception, we use the well-known tilt coordination technique [28]. By using this technique, linear sustained accelerations are artificially produced by tilting the platform. For the driver not to perceive the tilt, this one must be complemented by nontilting visual cues and under the rotation perception threshold [29]

$$f_x = a_x + g\sin(\theta). \tag{1}$$

The MCAs compared in this study use tilt coordination. Nevertheless, they depend directly on two fundamental MPC components: the mathematical model and the optimization.

A. Mathematical Model

1) DS Model: The DS dynamics is specific to the actuator manufacturers. Therefore, we chose to simplify the real system as a dual integrator model in order to access all simulator states such as the position p, the linear velocity v, the angle θ, and the angular speed ω of the platform along the x and y axes. This model does not consider the delays produced by the simulator mechanics and is represented by a linear time invariant system

$$\begin{aligned} x_{\text{DS}}(k+1) &= \overbrace{\begin{bmatrix} 1 & t_s & 0 & 0 \\ 0 & 1 & 0 & 0 \\ 0 & 0 & 1 & t_s \\ 0 & 0 & 0 & 1 \end{bmatrix}}^{A_{\text{DS}}} \overbrace{\begin{bmatrix} p(k) \\ v(k) \\ \theta(k) \\ \omega(k) \end{bmatrix}}^{x_{\text{DS}}(k)} + \overbrace{\begin{bmatrix} \frac{t_s^2}{2} & 0 \\ t_s & 0 \\ 0 & \frac{t_s^2}{2} \\ 0 & t_s \end{bmatrix}}^{B_{\text{DS}}} \overbrace{\begin{bmatrix} u_{\text{lin}} \\ u_{\text{rot}} \end{bmatrix}}^{u(k)} \\ y_{\text{DS}}(k) &= \overbrace{\begin{bmatrix} 0 & 0 & g & 0 \end{bmatrix}}^{C_{\text{DS}}} x_{\text{DS}}(k) + \overbrace{\begin{bmatrix} 1 & 0 \end{bmatrix}}^{D_{\text{DS}}} u(k) \end{aligned} \tag{2}$$

where $u(k)$ represents the linear u_{lin} and rotational u_{rot} accelerations. Instead of choosing acceleration as the tracking variable and output $y_{\text{DS}}(k)$, we choose the specific force (1), which explains why only x and y linear accelerations are considered to control the system. Model (2) is used for the M0 configuration.

2) Vestibular System Model: The DS model only considers simulator states while ignoring human motion perception. Then, aiming at improving simulation realism and drivers' immersion, a human vestibular system model is additionally integrated into the control design. This model is based on the vestibular system as it responds to head movements relative to gravity and space by using inertial-force receptors. The vestibular system detects linear and angular accelerations through different sensory organs: the otolith organs and the semicircular canals, respectively. Several authors have tried to represent, in a simplified way, the mechanisms of specific force sensation and angular velocity with a mathematical model [9]. The dead zone introduced by the detection of vestibular system's thresholds are not represented in the vestibular models presented in this work as they are treated as perceptive constraints in the optimization statement. The transfer function for the semicircular canals that links the perceived angular velocity $\hat{\omega}$ and the real angular velocity ω for the three rotations along the x, y, z axes is

$$\frac{\hat{\omega}}{\omega} = \frac{\tau_L \tau_a s^2 (1 + \tau_l s)}{(1 + \tau_a s)(1 + \tau_L s)(1 + \tau_s s)}. \tag{3}$$

This model is implemented as a filter for the three rotation angles. The result is then added to the tilt angles resulting from the optimization of the tilt coordination technique and then saturated to avoid exceeding the platform's physical limits.

For the otolith model, the relation between the specific force f and the sensed specific force $\hat{f}$ is

$$\frac{\hat{f}}{f} = \frac{G_o(\tau_{ao} s + 1)}{(\tau_{Lo} s + 1)(\tau_{so} s + 1)}. \tag{4}$$

Note that (1) refers to the specific force f along the x-axis

$$\hat{f}_x = \frac{G_o(\tau_{ao} s + 1)}{(\tau_{Lo} s + 1)(\tau_{so} s + 1)} \left[u_{\text{lin}}(s) + \frac{g}{s^2} u_{\text{rot}}(s) \right] \tag{5}$$

TABLE I
PARAMETERS OF VESTIBULAR MODELS

Model	Parameters							
	τ_L	τ_s	τ_l	τ_a	G_o	τ_{ao}	τ_{Lo}	τ_{so}
M1: [10], [11]	x: 6.1s y: 5.3s z: 10.2s	0.1s	0s	30s	0.4	13.2s	5.33s	0.66s
M2: [19]	5.73s	0.005s	0.06s	80s	0.4	10s	5s	0.016s

and is represented in the state-space form as

$$\dot{x_{\text{oto}}} = \overbrace{\begin{bmatrix} -T_3 & 1 & 0 & 0 \\ -T_4 & 0 & 1 & 0 \\ 0 & 0 & 0 & 1 \\ 0 & 0 & 0 & 0 \end{bmatrix}}^{A_{\text{oto}}} x_{\text{oto}} + \overbrace{\begin{bmatrix} T_1 & 0 \\ T_2 & 0 \\ 0 & gT_1 \\ 0 & gT_2 \end{bmatrix}}^{B_{\text{oto}}} \begin{bmatrix} u_{\text{lin}} \\ u_{\text{rot}} \end{bmatrix} \tag{6}$$

$$y_{\text{oto}} = \overbrace{\begin{bmatrix} 1 & 0 & 0 & 0 \end{bmatrix}}^{C_{\text{oto}}} x_{\text{oto}}$$

where

$$T_1 = \frac{G_o \tau_{ao}}{\tau_{Lo}\tau_{so}}, T_2 = \frac{G_o}{\tau_{Lo}\tau_{so}}, T_3 = \frac{\tau_{Lo} + \tau_{s0}}{\tau_{Lo}\tau_{so}},$$
$$T_4 = \frac{1}{\tau_{Lo}\tau_{so}}.$$

This system is used to minimize the motion perception error: the difference between the specific force perceived in the simulator and the one perceived in the vehicle. It is necessary to integrate the simulator system into the optimization reference model to add hard constraints on simulator states. Therefore, we unify the specific force system (6) and the DS system (2) to create the tilt coordination model

$$\dot{X_{\text{force}}} = \begin{bmatrix} A_{\text{oto}} & 0 \\ 0 & A_{\text{DS}} \end{bmatrix} \begin{bmatrix} x_{\text{oto}} \\ x_{\text{DS}} \end{bmatrix} + \begin{bmatrix} B_{\text{oto}} \\ B_{\text{DS}} \end{bmatrix} \begin{bmatrix} u_{\text{lin}} \\ u_{\text{rot}} \end{bmatrix}$$
$$Y_{\text{force}} = \begin{bmatrix} C_{\text{oto}} & 0 \end{bmatrix} \begin{bmatrix} x_{\text{oto}} \\ x_{\text{DS}} \end{bmatrix}. \tag{7}$$

This model (7) is implemented in the M1 and M2 strategies.

The parameters for both models are mostly based on subjective responses and may vary according to the literature. In this study, we analyze two of the most commonly used vestibular sensor models in MCAs: the one for M1 is the one proposed by Young–Oman/Meiry [10], [11] and the one for M2 is the one proposed by Telban and Cardullo [19]. The different parameters for each model are shown in Table I. In this table, $\tau_L/\tau_{\text{Loto}}$ are long time constants, $\tau_s/\tau_{\text{soto}}$ are short time constants, $\tau_a/\tau_{\text{aoto}}$ are adaptation operators, τ_l is a lead term to avoid vibration effects, and G_{oto} represents the static sensitivity for the otolith organs.

B. Optimization Statement

An MPC controller operates as an optimal tracking strategy that solves a specific optimization problem to obtain the desired reference trajectory for a finite control horizon N_u, within a prediction horizon N_p [30]. In this study, the cost function varies from one strategy to another. In the M0 configuration, the objective is to faithfully track the accelerations of the virtual vehicle, while in M1 and M2 configurations, the objective is oriented toward minimizing the error between the motion perceived in the simulator and the motion perceived in the virtual vehicle. In all three configurations, the cost function to be minimized is expressed as

$$J(k) = \sum_{j=0}^{N_p-1} \|r\,(k+j) - y(k+j)\|_\delta^2 + \|x\,(k+j)\|_q^2 + \sum_{j=1}^{N_u} \|\Delta u(k+j-1)\|_\lambda^2; \quad \text{s.t.} \quad A_c \Delta U \leq b \tag{8}$$

where δ, λ, and q are weighting parameters for the tracking error, the control, and the future states, respectively. r represents the reference trajectory that remains constant throughout N_p, and it takes the value of the specific force f for M0 and the perceived specific force $\hat{f}$ for M1 and M2 (see Section III-A for details). y and x represent the future output and future states of the system, respectively. Their values change according to the type of configuration, since they depend directly on the mathematical model. Δu is the decision variable and represents the rate of change of the rotational and linear acceleration. The matrix equation $A_c \Delta U \leq b$ represents the linear inequality constraints shown in Table III.

In order to solve the quadratic programming problem (8), the open-source tool qpOASES is implemented [31]. It applies the active set method and provides a ready-to-use package capable to find the optimal control action ΔU in real time.

TABLE II
WEIGHTING PARAMETERS

MCA	λ		q			δ
	Δu_{rot}	Δu_{lin}	x, $\dot{x}$, θ, ω	u_{rot}	u_{lin}	Error
M0	300	1	0	0.1	0.1	50/j
M1	100	0.2	0	0.1	0.01	80/j
M2	100	10	0	0.1	0.1	50/j

TABLE III
PLATFORM'S WORKSPACE AND PERCEPTIVE LIMITS

Limits	Displacement (m)	Velocity (m/s)	Acc. (m/s^2)
Hexapod	$x: 0.28/y: 0.26/z: 0.20$	0.7	7.5
Rails	2.6	$x: 2/y: 3$	5
Tilt/Pitch	$\theta: 5.5°/\phi: 5°$	$4°/s$	$8°/s^2$

C. Real-Time Execution

Several considerations must be taken into account to apply MPC-based MCA in real time (control frequency of 125 Hz) without presenting any risk to the platform or the user itself.

1) Control Tuning: Tuning consists in choosing the appropriate optimization and control parameters such as N_u, N_p, δ, λ, q and sample time to be applied in the cost function (8), in order to improve the system performance and ensure control feasibility. The perceptual and physical limits presented

in Table III are too restrictive and have influence on the region for which the optimization problem find a solution ΔU. Therefore, the weighting parameters were chosen in order to make the algorithm as efficient as possible for each configuration. We first applied a weighting unit value to the control variables Δu_{lin} and Δu_{rot}. However, it was not enough to ensure system closed-loop stability, and therefore, we use the trial-and-error method with a square signal of 2 m/s^2 at a frequency of 5 s. The selected parameters make the best compromise between the system closed-loop stability and the control strategy performance regarding trajectory tracking. They are presented in Table II.

When the platform is close to its limits in displacement, the simulator must slow down and return to a safe position without provoking any false cue, i.e., unwanted rendering of motion as a result of poor motion cueing or unexpected driving behavior [32]. To achieve this, we consider a suitable fair prediction horizon of six seconds. However, this value is very large considering real-time control frequencies as the optimization problem cannot be solved due to high computational costs. This problem was fixed using two different sampling times when creating the discrete-state-spaces forms, (2) and (7). The first sample time corresponds to the control frequency and was applied to the first ten steps. The second sample time was set to 0.3 s and was applied for 20 steps in order to reach the requested prediction time. In that sense, N_p takes 30-time steps. Another important parameter is the control horizon N_u that indicates the number of parameters used to capture the future control trajectory ΔU for all configurations. Important N_u values can leave to high computational loads, but small ones can result on closed-loop instability. We decided to make a tradeoff between both aspects by setting the control horizon at 3-time steps.

2) Stability: Traditionally, tuning parameters are enough to ensure closed-loop stability and performance in MPC [33]. Nevertheless, in the presence of state constraints, MPC becomes difficult to control and closed-loop stability will depend on the optimal solution over N_p, i.e., problem (8) needs to be feasible to satisfy the limits. In this study, we used two different approaches to ensure closed-loop stability. The first one consists in introducing a terminal penalty matrix equal to the solution of the discrete algebraic Riccati equation used in the infinite horizon cost function [34]. This condition implies that the cost function is Lyapunov and then, when feasibility is verified, nominal stability is guaranteed for the MPC system in closed loop. Additionally, it restricts severely the system and is not enough to guarantee a feasible solution along N_p. Hence, we use an additional stability condition proposed by [27]. Their approach proposes a braking law for the linear (9) and angular (10) signals, in which, once the simulator approaches its physical limits, it returns to its neutral position with a certain acceleration threshold. This law is transformed in terms of ΔU and is applied as hard constraints in (8)

$$p_{\min} \leq p_k + c_v T v_k + \frac{T^2 u\text{lin}_k}{2} \leq p_{\max} \tag{9}$$

$$\theta_{\min} \leq p_k + c_v T \dot{\theta} + \frac{T^2 u\text{rot}_k}{2} \leq \theta_{\max} \tag{10}$$

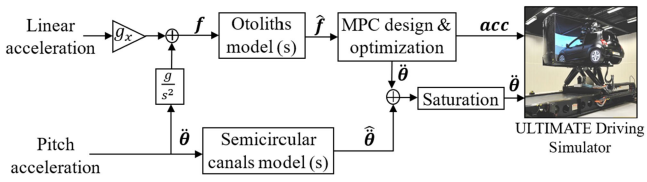

Fig. 1. Control design for the DS's movement restitution based MPC along the x-axis.

where $c_v = 1.9$ and $T = 1.6$ are tuning parameters allowing the feasible optimization solution over the prediction horizon.

III. Motion Strategies Comparison

This section describes the differences between the three considered MCAs from a theoretical and experimental viewpoints.

A. General Framework

The three motion configurations M0, M1, and M2 implement the same control design for linear and angular accelerations. Fig. 1 illustrates the complete MPC-based MCA framework for accelerations along the x-axis, in which the input signals are linear and angular accelerations from the vehicle dynamic model, which takes as inputs the signals sent from the simulator's pedals and steering wheel.

Considering that tracking the full input signal is not necessarily the best solution for self-motion perceived coherence in motion restitution, the input signals have been scaled down according to each configuration. A study conducted by Berthoz *et al.* [35] showed that MCA lower unit gains comprised between 0.4 and 0.75 give more perceived coherence of self-motion and provide a better optimization of the actuators working space. Hence, we selected a 0.6 gain g_x for scaling the specific force signal f. The same value was implemented along the y-axis as it provides balance between visual and vestibular attention [36].

Since strategy M0 does not incorporates the vestibular system, the blocks that represent the transfer function for otolith organs and semicircular canals models are included only for M1 and M2 configurations. For instance, when using M0, these blocks are replaced with a unit gain. Once the signals are scaled down, MPC-based optimization is performed, resulting in some optimal values of linear and angular accelerations.

The saturation block represents a high-pass filter aiming at saturating the angular acceleration input signal coming from the vehicle model behavior in terms of angular position and velocity, while keeping the platform within its physical limits. Details about the simulator are presented in Section IV-B.

B. Theoretical Analysis

The differences between both vestibular system models, M1 and M2 come from the parameter values in the transfer functions for the semicircular canals (3) and the otolith organs (4). As a consequence, both models behave as different acceleration filters. These values are shown in Table I. Regarding the otolith model (4), Fig. 2 shows the frequency response of

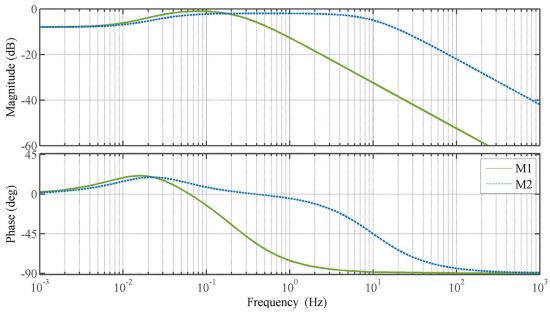

Fig. 2. Frequency response of the otolith models proposed by Young–Oman/Meiry (M1) and Telban (M2).

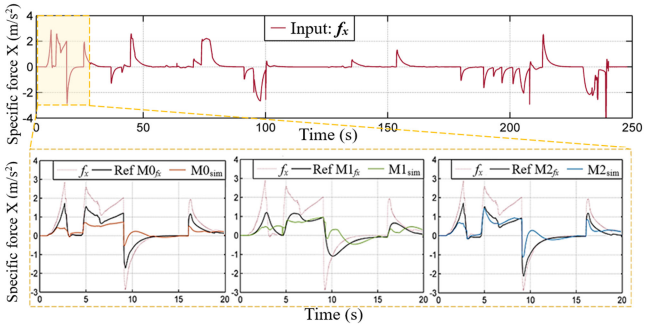

Fig. 3. Motion restitution according to each configuration: the top image is the autonomous vehicle acceleration signal along the x-axis F_x; the plots from the left to the right are the tracking signal with model M0, with the M1 model, and with the M2 model. Each of these three figures show the F_x, the scaled F_x, and the DS tracking response for M0, M1, and M2.

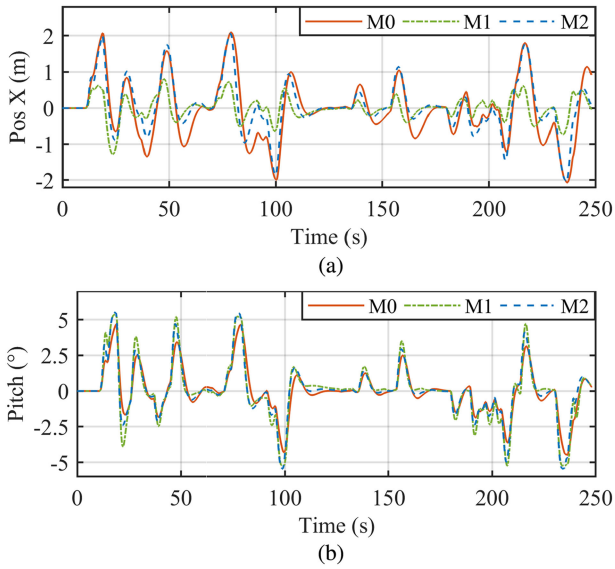

Fig. 4. Comparison between the longitudinal platform's position (a) and pitch angle (b) for strategies M0, M1, and M2.

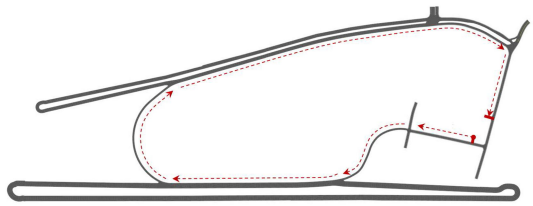

Fig. 5. Terrain and paths used for the DS tests.

Young–Oman/Meiry's [11] and Telban and Cardullo's [19] models for the acceleration input along the x and y axes. In the magnitude diagram, we can see that none of the models represents a signal amplification, in contrast, both models tend to attenuate the input signal and to act as low-pass filters, with a higher magnitude for the M2 model. For M1, the otolith's sensitivity is higher between 0.03 and 0.2 Hz, and higher between 0.06 and 5 Hz for M2. This indicates that M2 covers all the frequency range of the most normal head movements from 0.1 to 1 Hz [37].

In this study, the semicircular canals model (3) is used only as a rotational accelerations filter that come directly from the vehicle model. Therefore, this mode is not present on the MPC mathematical model for any of the configurations, M1 and M2. For this reason, there is no theoretical analysis of the semicircular canals model. In addition, the phase and magnitude values for M1 and M2 semicircular models act in the range of normal head motion [19] for both models. The M0 configuration is not compared in this section as it tracks the acceleration input signals completely without integrating any filter, as explained earlier in the MPC framework.

C. Tracking Performance Analysis

To understand how each configuration restores motion, we used the data collected after driving the simulator in an AD mode, using the terrain scenario presented in Fig. 5. The result is a signal containing transient and continuous accelerations that last 250 s. This input signal is referenced as Input: f_x in Fig. 3 and represents the autonomous vehicle behavior along the x-axis.

The remaining three curves in Fig. 3 show motion restitution in a 25-s zoom section to enable tracking legibility for each configuration M0, M1, and M2. The specific force f_x is the input signal for all configurations, as illustrated in each plot. Nevertheless we scaled it differently for each configuration to obtain the sensed specific force input $\hat{f}$ for M1 and M2 after passing the otolith model or simply the same signal with a lower gain g_x in the M0 configuration.

None of the three configurations reaches one-to-one tracking motion as the physical and perceptive limits were very restrictive. The M1 configuration does not restore well transient accelerations and invests much energy in the platform's continuous accelerations that were generated by tilting the cockpit. This fact generates a higher phase lag in motion restitution since the maximum angular speed was $4°/s$. This value was selected according to the study developed by Fang *et al.* [38]. All perception and physical limits implemented in this study are presented in Table III.

To analyze objectively the specific force restored by the simulator of each configuration, we collected the longitudinal acceleration and the tilting angle data for the breaking scenario test that occurs approximately after 8 s of simulation. This

TABLE IV
BREAKING VALUES COMPARISON

MCA	$\min_\theta(^\circ)$	$\min_{ax}(m/s^2)$	$\min_{fx}(m/s^2)$	$\min_{Jx}(m/s^3)$	$\Delta t(s)$
M0	1.65	-0.63	-0.54	-74.78	0.008
M1	3.90	-0.41	-0.47	-70.09	0.232
M2	2.40	-1.08	-1.12	-113.39	0.016

use case was selected since it requires a significant effort of specific force tracking. In Table IV, we report the minimum values of the different parameters such as the inclination angle θ, the longitudinal acceleration ax, the specific force fx, and the jerk Jx. We also included the difference in time occurrence Δt between the peak in specific force for each strategy and the vehicle data. It can be observed that in terms of longitudinal acceleration amplitude, M2 leads to a higher value than the other configurations since it mainly restores high acceleration frequencies. Additionally, M2 is less smooth than the others as it presents the highest value of Jx. The θ from M1 has a greater amplitude as it tracks more the low-frequency (LF) accelerations than the others. Regarding Δt, the M0 strategy is the fastest, followed by M2 and M1.

The tracking task performance is linked with the simulator's workspace. Fig. 4(a) shows the x rail displacement when using the three different MCAs. The M0 and M2 strategies mostly use all parts of the workspace, while the M1 strategy only uses half of the available space. Indeed, the M1 model filters the high frequencies accelerations, which are mostly restored by the simulator's rails. However, the LF accelerations obtained by tilting the simulator are more restored by the M1 strategy than with M0 or M2 as can be seen in Fig. 4(b).

IV. EXPERIMENTAL METHODOLOGY

A. Participants

For this experiment, we recruited 41 Renault employees. All participants (mean age: 36.6 years, SD age: 11.5 years) had a driving license and signed a consent form. Three participants were unable to complete the test as they felt symptoms of simulator sickness during the experiment. Therefore, 38 participants were included in the data analysis. Participants were separated into two groups depending on the driving mode. The first one with 19 subjects drove the simulator actively in a free mode, while for the last 19 subjects, the simulator behaved as a self-driving vehicle.

B. Driving Simulator

We used the ULTIMATE simulator, which was built in 2004 by Renault. It is an eight degree-of-freedom high-performance DS composed of a hexapod platform and linear rails [39]. The motion envelope given by the hexapod and the rails are detailed in Table III. The visual scene was displayed on a cylindrical screen covering a horizontal field of view of 210°. The cockpit is composed of a manual gearbox, steering force feedback, and a sound system reproducing engine and environmental noises.

C. Procedure

We conducted the experiment in different steps. Upon arrival to the simulator, all participants completed a preliminary information sheet and signed a consent form. Then, they were explained the procedure and safety instructions. Regardless of the driving mode, participants were asked to pay attention to the platform movement in each use case (stop/go situations, slalom, etc.) that were presented during the simulation.

After a familiarization driving test that lasted between 150 and 200 s, two different groups were designated randomly. The first group named FD*mode* consisted of 19 participants who passed the three configurations (M0, M1, M2) with full control of the vehicle. The second group named AD*mode* was composed of 19 participants who did the test using a simulated self-driving vehicle. We made two different groups to find out whether the MCA should be adapted depending on the driving modes and, in that case, analyze the impact of the vestibular system model on MCA adjustments for the AD or FD modes. Each subject drove the DS four times including the familiarization phase and the three MCAs. For the group that drove the simulator in the FD mode, there were traffic signs and verbal instructions in the familiarization phase indicating the speed limit and the path. Between each drive, participants were asked to complete a motion cueing questionnaire (see Section IV-C2). For one subject, the entire experiment took approximately one hour to complete. After the four driving tests, the subjects were asked to rank in order of preference the three configurations indicating first the best one.

1) Test Scenario: The study was conducted in a simulation environment generated with the SCANeR Studio driving simulation software.[1] SCANeR Studio also served to create the self-driving vehicle and the road environment use cases used for the comparison between motion strategies. The terrain is shown in Fig. 5. It was wilfully generated with segments including a city, a highway, and merging sections aiming at producing inputs simulator signals, especially high-frequency (HF) and LF accelerations, as follows.

HFx : transient x accelerations, e.g., stop/go situations.
LFx : continuous x accelerations, e.g., highway use cases.
HFy : transient y accelerations, e.g., slalom use case.
LFy : continuous y accelerations, e.g., merging sections.

HFx signals were presented mostly at the beginning of the experiment and correspond to the section between 0 and 50 s in Fig. 6(a). LFx signals are illustrated in the section between 75 and 90 s in the same figure. The generic slalom driving scenario consisted of a series of obstacles aligned on a two-line straight road. The maximal speed in this road segment was fixed to 70 km/h, generating a sine-like trajectory with a maximal lateral acceleration of 1 m/s^2. This use case is shown in Fig. 6(b) between 130 and 180 s. The last type for continuous y accelerations are shown in Fig. 6(a) between 40 and 60 s and between 100 and 175 s.

The self-driving vehicle implemented for the AD mode was designed by a script-based controller capable of handling all

[1] https://www.avsimulation.com/

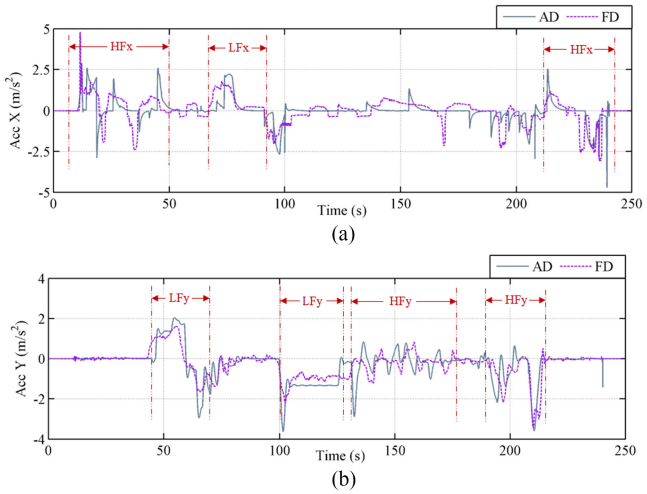

Fig. 6. Accelerations comparison between the AD and the FD modes, after driving the test (a) along the longitudinal x-axis and (b) lateral y-axis: the AD signals corresponds to the autonomous vehicle model accelerations signals and the FD signals corresponds to a random participant accelerations signals.

TABLE V
MOTION RATING SCALE FOR EACH SIGNAL TYPE

Attribute	Rating	
	1	7
Smoothness	Same as fixed platform	Extremely jerky
Sense	Correct as in the real car	Totally inverse
Amplitude	No motion experienced	At least twice that expected
Delay	None experienced	Unacceptable
Discomfort	None experienced	Cannot continue the test
Disorientation	None experienced	Cannot perform maneuvers

planning decisions and different use cases safely. Most of self-driving actions depended on the autonomous behavior provided by the traffic model from the simulation software.

The driving behavior of the AD model was compared with the acceleration signals of one random participant after driving the scenario test. The results are shown in Fig. 6(a) and (b). In Fig. 6(b), we can observe that lateral accelerations follow the same path and frequencies in both free and AD modes. Indeed, they depend mainly on the trajectory imposed by the terrain and not necessarily on the driver command inputs. Besides, the longitudinal trajectories along the x-axis [see Fig. 6(a)] are slightly different, especially for positive transient accelerations. This effect depended in one hand on the drivers' anticipation and driving style, and on the other hand, on the vehicle dynamic model. The presence of lag in the curves is explained by different speeds profiles when driving the simulator, as they were controlled by different driving modes.

2) Motion Cueing Questionnaire: After each drive on the simulator, participants filled out the motion rating scales index [40] that evaluates the following different MCA characteristics: smoothness, sense (motion perception), delay, amplitude, discomfort, and disorientation for each of the the following four situations: acceleration/braking, long turns, slalom, and continuous acceleration. For each situation named earlier, subjects had to score from 1 to 7 according to Table V.

In the last part of this questionnaire, participants scored the MCA using a seven-point Likert scale (1: "strongly disagree"; 7: "strongly agree") [35]. Three statements had to be scored: "I forgot the simulator," "Motion was realistic, I felt like I was driving," and "I drove as usual" (in the FD mode only).

V. EXPERIMENTAL RESULTS AND DISCUSSION

The analysis was based on the MCA questionnaire scores provided by each participant. Two different tests were carried out: the first one consisted in comparing the MCA characteristics within-subject (see Section IV-C2) among the three configurations (M0, M1, M2). Each feature of each configuration was grouped within a pair, e.g., Amplitude: M0 with M1; M1 with M2, and M0 with M2. This analysis was made with the data of 19 participants who drove the simulator in FD mode and the 19 participants who drove in AD mode. The second test compared by MCA, the features between the AD and the FD modes, i.e., Amplitude: M0-free with M0-auto; M1-free with M1-auto, and M2-free with M2-auto. In this case, the test was between-subject as the populations to be compared were different. All results and figures shown from now on correspond only to the data that are statistically significant different in at least one of the analyzes, not to overload this article.

A. Driving Mode

All MCA characteristics have been tested for normality using the Shapiro–Wilk test. No distribution was found to be normal, therefore, we used nonparametric paired Wilcoxon signed-rank tests with a significance level of 5%, in order to determine whether or not, there were significant differences between all MCAs characteristics of each configuration (M0, M1, M2). Three separate Wilcoxon signed-rank tests (corresponding to the three configurations) were done for each characteristic. Hence, we applied a Bonferroni correction leading to a significance level of: $p < 0.05/3 = 0.016$. The study considered separately the 19-person group for the AD mode and the 19-person group for the FD mode.

1) Group One: FD Mode: The test showed that continuous accelerations along both x and y axes presented significant differences: along the x-axis, the Delay attribute with M1 was greater than with M2 ($Z = 2.18, p = 0.014$); along the y-axis, the delay using M0 was less important than the one perceived using M1 ($Z = 2.18, p = 0.015$). In both cases, M1 presented a greater delay score when compared with the other two configurations regarding continuous accelerations. We can explain this result by analyzing the M1 tracking task: when applying the M1 otolith organs model in an MPC framework, HF accelerations are filtered out. Consequently, when minimizing the perceptive error of the specific force, angular accelerations and thereby tilt angles have more weight than linear accelerations. However, the angular speed threshold generates a signal delay when tilt angles are important. In line with this result, we can observe in Table IV that for a braking use case, the M1 Δt is greater than the one obtained with the other two strategies. Although the Δt between M0 and the others strategies was not substantial, i.e., about 0.2 s, it was high enough to be noticed by the participants as a delay.

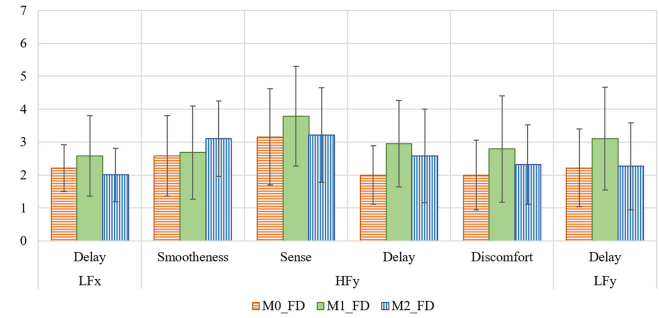

Fig. 7. Mean and SD for the MCA features with a statistically significant difference using the FD mode condition.

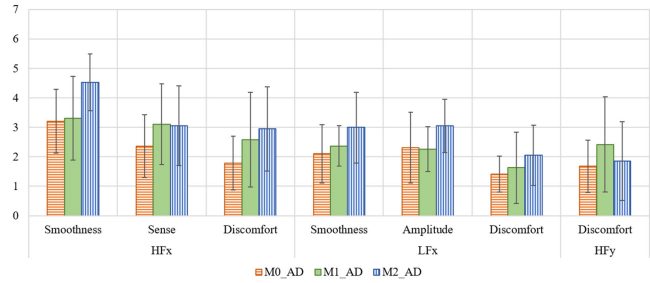

Fig. 8. Mean and SD for the MCA features with a statistically significant difference in the AD mode condition.

The M1 delay attribute score was also greater in the slalom use case when comparing M0 and M1 ($Z = 2.39, p = 0.009$). In the same use case, M2 presented a greater delay value than the M0 strategy ($Z = 2.16, p = 0.015$).

Among other features, in the slalom use case more differences were found between the configurations: the M0 strategy was smoother than M2 ($Z = 2.31, p = 0.011$); Sense was almost inverted using M1 instead of M2 ($Z = 2.35, p = 0.009$), and Discomfort attribute was less noted with M0 than M1 ($Z = 2.35, p = 0.009$). Participants found the M0 and M1 strategies smoother than M2. This may be due to the tracking performance of strategy M2, as it privileges transient accelerations allowing for greater signal jerk. In fact, HF accelerations and jerk can contribute significantly to the perceived strength of motion and are important in vehicle speed estimation [41]. Without them, drivers could feel a different movement from what they expected, as observed using the M1 strategy. However, despite being an important parameter, we cannot conclude in this experiment, whether or not, jerk improves the motion perception of the simulator. It should also be noted that jerk is affected by the weighting parameter λ in the cost function (8), since for the M0 strategy, this was more penalized to allow feasibility of the optimization problem overall N_p.

One unexpected finding is that no significant difference was found for transient accelerations along the x-axis, even though motion restitution for this type of signal was considerably different for the three configurations, as shown in Fig. 3. Fig. 7 summarizes the means and standard deviations for the characteristics with statistically significant differences.

2) Group Two: AD Mode: Compared with the FD mode, there were more differences between characteristics, notably the acceleration components along the x-axis. For HF accelerations, the M2 strategy was less smooth compared to M0 ($Z = 3.32, p = 0.0004$) and M1 ($Z = 2.92, p = 0.002$); motion perception was better with strategy M0 in contrast with the strategies including a vestibular model, either M1 ($Z = 2.07, p = 0.018$) and M2 ($Z = 2.24, p = 0.001$); Discomfort was greater with M1 ($Z = 2.31, p = 0.010$) and M2 ($Z = 2.76, p = 0.003$) when compared to M0, but there was not a significant difference between M1 and M2. For LF accelerations, M0 was still smoother ($Z = 2.68, p = 0.004$) and more comfortable ($Z = 2.18, p = 0.014$) than M2, and the M2 Amplitude was larger compared to M0 ($Z = 2.15, p = 0.015$) and M1 ($Z = 2.62, p = 0.004$). These results show that the M2 strategy is more aggressive than M0 and M1, for both low and high frequencies, which is consistent with the M2 motion tracking for transient accelerations, but not for low frequencies. This may imply that participants did not distinguish between the two types of frequencies, making their opinion biased by the high frequencies. Hence, in general, participants felt the M2 motion restitution along x jerkier than normal driving, which is in accordance with the objective data shown in Table IV for Jx. Overall, the M0 strategy was the most appreciated for motion cueing along the x-axis as it scored better in comfort and movement perception compared to the strategies using a vestibular model in the control loop design. Only one difference was found along the y-axis: Discomfort was greater for HF accelerations when using M1 rather than M0 ($Z = 2.12, p = 0.016$). Fig. 8 shows the comparison between the parameters with statistically significant differences for the AD mode group and the means and standard deviations for each parameter. In short, participants preferred the characteristics provided by the M0 strategy rather than strategies integrating a vestibular system model. This can be explained by the self-driving vehicle model. As explained before, the model was based on a script controller that reacts for different use cases, in which the acceleration profile depends on the traffic model provided by the SCANeR studio software as well as the vehicle model dynamics. Transient accelerations were perceived aggressively, and therefore, the M0 MCA scored better than the other two strategies, as it makes a correct balance between HL and LF accelerations.

B. Autonomous Versus FD mode

In this part, we evaluate the differences between characteristics of the different groups, free and AD modes. To do this, nonparametric Mann–Whitney tests were used as there were different populations. The means and standard deviations for each characteristic that were statistically significant different between both groups are shown in Fig. 9. We can see that there is a difference in all situations, at least in sense, disorientation, and delay. For these characteristics, subjects tended to rate more badly the FD mode than the AD mode. We believe that this result comes from a comparison between participants' usual driving behavior in real life and the simulator motion. Currently there is no reference for AD and consequently, participants tended to evaluate the AD mode instead of the simulator motion cues. This

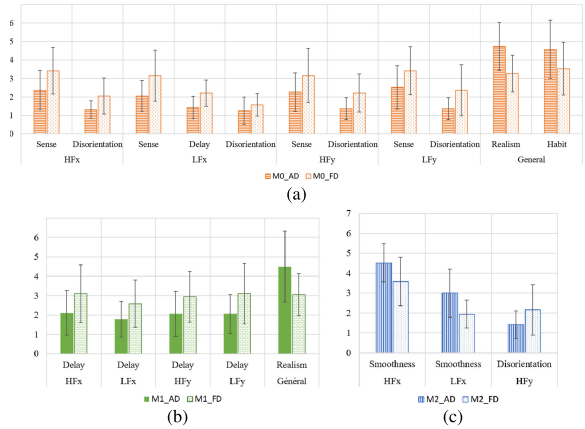

Fig. 9. Mean and SD for the MCA features with statistically significant differences between the autonomous and the FD modes: (a) strategy M0, (b) strategy M1, and (c) strategy M2.

effect is salient when considering the M0 strategy: in the AD mode, M0 was better appreciated than the other two strategies concerning motion perception and orientation, however, in the FD mode M0 did not stand up among M1 and M2. Another observation that supports this hypothesis is the difference in smoothness for the M2 configuration, i.e, in the AD mode, this configuration was scored as aggressive, nevertheless in FD, the M2 motion cueing was consistent with continuous and transient accelerations, and in general, participants preferred this strategy better than M1.

One of the limitations of the study is the disparity between subjects shown in the standard deviations for most situations. This means that part of the population had different opinions for each strategy. However, this result was expected given the subjectivity of the experiment. Another consideration is the influence of drivers' adaptation to the simulator. Unfortunately, based on the simulator and participants availability, all three strategies were presented consecutively and randomly. Furthermore, the motion control strategy for this experiment can influence the drivers' motion perception, and thus, their subjective answers. Indeed, motion restitution was mainly based on the tracking of the specific force. To obtain the specific force, we used the tilt coordination technique, which combines rotational and translational motion of the platform. However, if this technique is not correctly implemented, it may generate an inaccurate motion perception, as it does not correspond to a natural driving movement. In addition, other studies have shown that the tilt perception thresholds must be adapted according to the level of acceleration to improve realism [3]. This leads us to believe that some participants may have been influenced not only by the type of model used in each strategy but also by the cueing strategy itself. Moreover, the final perception of the movement may be influenced not only by the stimuli of the vestibular system, but also by the multisensory integration.

According to the last part of the questionnaire presented in Section IV-C, seven participants preferred the M0 strategy and 12 participants preferred the M2 strategy which, in addition to the dynamics of the platform, integrates the human perception model. No participant chose the M1 strategy.

VI. Conclusion and Future Work

This study described a driver-in-the-loop experiment in a DS. Three strategies were compared using a real-time implementation of MPC-based MCA. The strategies depended on the mathematical model used in the control-loop design: the first one named M0 corresponded to the platform's dynamic model. The other two strategies additionally integrated Young–Omang/Meiry's and Telban and Cardullot's vestibular sensor models, named M1 and M2, respectively. The experiment compared an AD and a FD mode. The study focused mainly on motion perception for x–y HF and LF accelerations. Results showed that the mathematical model has an impact on the MCA restitution for both axes of movement. In FD mode, M2 strategy showed appropriate behavior in lateral motion since the other two were significantly smoother, e.g., inhibiting motion perception in the slalom use case. Besides, M1 configuration was the least desired in this category since the simulator movement did not correspond to a real driving compared to the M2 strategy, and it was less comfortable than driving with the M0 strategy. Also, in the discussion with the participants, the majority considered that it was difficult to adapt to this strategy, even though it was presented in a random order. They agreed that the movement, in addition to being perceived with a delay, was inconsistent with the visual environment. Moreover, we cannot assume that M2 is the best strategy regarding motion perception as further research is needed to conclude on the advantages of implementing the M2 vestibular system model over only the simulator's model of M0.

Regarding the AD mode, we found that participants preferred motion cueing provided by the M0 model as it offered less discomfort, delay, and better simulation immersion than using a vestibular system model. We believe that the strategies rating was quite affected by the acceleration profile provided by the autonomous vehicle behavior, which presented an instantaneous response regarding transient accelerations, especially along the x-axis. In this sense, configuration M2 was considered as too aggressive in the AD mode as it restored more HF accelerations compared to M0 and M1. The M1 strategy, on the other hand, was not qualified as very aggressive, but participants noticed discomfort and a wrong perception of movement when using it. The delay attribute was less important in both modes for MCA M0. One reason is that the additional vestibular system filters for M1 and M2 strategies generates an additional time delay. When comparing both driving modes, several differences were found, especially regarding strategy M0. This indicates that it is necessary to re-evaluate the AD mode and compare the types of driving.

Summarizing all results, we can conclude that regardless of the driving mode, the M1 strategy is the least preferred by participants. This fact is explained by the lack of restitution of transitory accelerations among others, a condition highly necessary in MCAs since the perception of speed, the conditions of the road and the vehicle behavior depend on it. Results provide further evidence of the imperative need to select an appropriate mathematical model to define the tracking task in MPC-based MCA control design and the importance of including driver-in-the-loop feedback to develop higher degree of realism and accurate motion cues.

In this study, we only considered the subject's motion perception on the specific force. Therefore, to deeply understand the drivers' appreciation of the overall motion experience, we could employ a continuous real-time evaluation for all degrees of freedom as proposed in [42]. Future research will also look into a deeper comparison between the M0 and M2 configurations using larger and more representative populations. Additionally, we will take into account the driving performance in order to give an objective analysis to this study. We will also deploy a self-driving model with human-like driving characteristics to provide a more realistic and immersive simulator's virtual driving environment. Driving behavior is an important factor that must be considered when defining an MCA as it can influence the way subjects perceive movement in real life as well as in a DS.

REFERENCES

[1] R. A. Wynne, V. Beanland, and P. M. Salmon, "Systematic review of driving simulator validation studies," *Saf. Sci.*, vol. 117, pp. 138–151, Aug. 2019.

[2] E. K. Orhorhoro, A. E. Ikpe, and G. Abdulsamad, "Performance evaluation of simulated motion cueing algorithm of a driving simulator," *Amer. Int. J. Res. Sci., Technol., Eng. Math.*, vol. 16, no. 1, pp. 5–12, 2016.

[3] A. Stratulat, V. Roussarie, J.-L. Vercher, and C. Bourdin, "Improving the realism in motion-based driving simulators by adapting tilt-translation technique to human perception," in *Proc. IEEE Virtual Reality Conf.*, Mar. 2011, pp. 47–50.

[4] A. Nesti, S. Nooij, M. Losert, H. H. Bülthoff, and P. Pretto, "Roll rate perceptual thresholds in active and passive curve driving simulation," *Simulation*, vol. 92, no. 5, pp. 417–426, May 2016.

[5] H. Asadi, S. Mohamed, C. P. Lim, and S. Nahavandi, "A review on otolith models in human perception," *Behav. Brain Res.*, vol. 309, pp. 67–76, Aug. 2016.

[6] F. Colombet, Z. Fang, and A. Kemeny, "Tilt thresholds for acceleration rendering in driving simulation," *Simulation*, vol. 93, no. 7, pp. 595–603, Jul. 2017.

[7] H. Asadi, S. Mohamed, K. Nelson, and S. Nahavandi, "A linear quadratic optimal motion cueing algorithm based on human perception," in *Proc. Australas. Conf. Robot. Autom.*, 2014, pp. 1–9.

[8] Z. Fang and A. Kemeny, "Review and prospects of renault's MPC based motion cueing algorithm for driving simulator," in *Proc. Driving Simul. Conf.*, 2014, pp. 23–32.

[9] A. Q. Momani and F. M. Cardullo, "A review of the recent literature on the mathematical modeling of the vestibular system," in *Proc. AIAA Model. Simul. Technol. Conf.*, Jan. 2018, pp. 1–35.

[10] L. R. Young and C. M. Oman, "Model for vestibular adaptation to horizontal rotation," *Aerosp. Med.*, vol. 40, pp. 1076–1080, 1969.

[11] L. R. Young and J. L. Meiry, "A revised dynamic otolith model," *Aerosp. Med.*, vol. 39, no. 6, pp. 606–608, 1968.

[12] G. L. Zacharias, "Motion cue models for pilot-vehicle analysis," DTIC document, Fort Belvoir, VA, USA, Tech. Rep. ADA061477, 1978.

[13] L. Reid and M. A. Nahon, "Flight simulation motion-base drive algorithms: Part 1. developing and testing equations," Univ. Toronto, Toronto, ON, Canada, Tech. Rep., no. 296. 1985.

[14] B. D. C. Augusto, "Motion cueing in the Chalmers driving simulator: An optimization-based control approach," Masters thesis, Dept. Mech. Eng.,Tech. Univ. Lisbon, Lisboa, Portugal, 2009.

[15] S.-H. Chen and L.-C. Fu, "An optimal washout filter design for a motion platform with senseless and angular scaling maneuvers," in *Proc. Amer. Control Conf.*, 2010, pp. 4295–4300.

[16] N. J. Garrett and M. C. Best, "Model predictive driving simulator motion cueing algorithm with actuator-based constraints," *Veh. Syst. Dyn.*, vol. 51, no. 8, pp. 1151–1172, 2013.

[17] H. Asadi, S. Mohamed, and S. Nahavandi, "Incorporating human perception with the motion washout filter using fuzzy logic control," *IEEE/ASME Trans. Mechatronics*, vol. 20, no. 6, pp. 3276–3284, Dec. 2015.

[18] A. Lamprecht, D. Steffen, J. Haecker, and K. Graichen, "Comparison between a filter and an MPC-based MCA in a offline SImulator study," in *Proc. Driving Simul. Conf.*, 2019, pp. 101–107.

[19] R. J. Telban and F. M. Cardullo, "Motion cueing algorithm development: Human-centered linear and nonlinear approaches," NASA, Washington, DC, USA, Tech. Rep. NASA/CR-2005-213747, 2005.

[20] K. Zaychik, F. Cardullo, G. George, and L. Kelly, "Evaluating effectiveness of modeling motion system feedback in the enhanced hess structural model of the human operator," in *Proc. AIAA Conf. Model. Simul. Technol.*, Aug. 2009, pp. 1–14.

[21] M. Baseggio, A. Beghi, M. Bruschetta, F. Maran, and D. Minen, "An MPC approach to the design of motion cueing algorithms for driving simulators," in *Proc. 14th Int. IEEE Conf. Intell. Transp. Syst.*, 2011, pp. 692–697.

[22] A. Beghi, M. Bruschetta, and F. Maran, "A real time implementation of MPC based motion cueing strategy for driving simulators," in *Proc. 51st Conf. Decis. Control*, 2012, pp. 6340–6345.

[23] A. Mohammadi, "Enhancing human motion perception in model predictive motion cueing algorithm," Ph.D. dissertation, Deakin Univ., Geelong, VIC, Australia, 2018.

[24] H. Asadi, S. Mohamed, C. P. Lim, and S. Nahavandi, "Robust optimal motion cueing algorithm based on the linear quadratic regulator method ANS and a genetic algorithm," *IEEE Trans. Syst., Man, Cybern. Syst.*, vol. 47, no. 2, pp. 238–254, Feb. 2017.

[25] M. Bruschetta, C. Cenedese, and A. Beghi, "A real-time, MPC-based motion cueing algorithm with look-ahead and driver characterization," *Transp. Res. Part F: Traffic Psychol. Behav.*, vol. 61, pp. 38–52, Feb. 2019.

[26] M. Dagdelen, G. Reymond, A. Kemeny, M. Bordier, and N. Maïzi, "Model-based predictive motion cueing strategy for vehicle driving simulators," *Control Eng. Pract.*, vol. 17, pp. 995–1003, 2009.

[27] Z. Fang, M. Tsushima, E. Kitahara, N. Machida, D. Wautier, and A. Kemeny, "Motion cueing algorithm for high performance driving simulator using yaw table," *IFAC-PapersOnLine*, vol. 50, no. 1, pp. 15965–15970, Jul. 2017.

[28] B. Conrad and S. Schmidt, "Motion drive signals for piloted flight simulator," Inc. Palo Alto, CA, US, Contractor Rep. NASA-CR-1601, 1970.

[29] G. Reymond and A. Kemeny, "Motion cueing in the renault driving simulator," *Veh. Syst. Dyn.*, vol. 34, pp. 249–259, Oct. 2000.

[30] C. Bordons and E. Camacho, *Model Predictive Control*. London, U.K.: Springer-Verlag, 2007.

[31] H. J. Ferreau, C. Kirches, A. Potschka, H. G. Bock, and M. Diehl, "qpOASES: A parametric active-set algorithm for quadratic programming," *Math. Program. Comput.*, vol. 6, no. 4, pp. 327–363, 2014.

[32] P. Hansson and A. Stenbeck, "Prepositioning of a driving simulator motion system," *Int. J. Veh. Syst. Model. Testing*, vol. 10, no. 3, pp. 288–304, 2015.

[33] L. Wang, *Model Predictive Control System Design and Implementation Using MATLAB (Advances in Industrial Control)*. Berlin, Germany: Springer, 2009.

[34] W. H. Kwon, A. M. Brucktein, and T. Kailath, "Stabilizing state-feedback desing via the moving horizon method," *Int. J. Control*, vol. 37, no. 3, pp. 631–643, 1983.

[35] A. Berthoz *et al.*, "Motion scaling for high-performance driving simulators," *IEEE Trans. Human-Mach. Syst.*, vol. 43, no. 3, pp. 265–276, May 2013.

[36] J. Greenberg, B. Artz, and L. Cathey, "The effect of lateral motion cues during simulated driving," in *Proc. Driving Simul. Conf.*, 2003, pp. 8–10.

[37] L. R. Young, "Perception of the body in space: Mechanisms," in *Handbook of Physiology: The Nervous System*, vol. 3, R. Terjung, Ed. Hoboken, NJ, USA: Wiley, 1984, pp. 1023–1066.

[38] Z. Fang, F. Colombet, J.-C. Collinet, A. Kemeny, and I. S. Center, "Roll tilt thresholds for 8 DOF driving simulators," in *Proc. Driving Simul. Conf. Europe*, Paris, France, 2014, pp. 4–5.

[39] M. Dagdelen, J.-C. Berlioux, F. Panerai, G. Reymond, and A. Kemeny, "Validation process of the ULTIMATE high-performance driving simulator," in *Proc. Driving Simul. Conf.*, 2006, pp. 37–48.

[40] R. B. Sullivan, "The use of vestibular models in flight simulator motion washout systems: An experimental evaluation," Ph.D. dissertation, Dept. Aeronaut. Astronaut., Massachusetts Inst. Technol., Cambridge, MA, USA, 1985.

[41] B. Haycock and P. R. Grant, "The influence of jerk on perceived simulator motion strength," in *Proc. Driving Simul. Conf. North Amer.*, Iowa, 2007, pp. 1–11.

[42] D. Cleij, J. Venrooij, P. Pretto, D. M. Pool, M. Mulder, and H. H. Bulthoff, "Continuous subjective rating of perceived motion incongruence during driving simulation," *IEEE Trans. Human-Mach. Syst.*, vol. 48, no. 1, pp. 17–29, Feb. 2018.